PERGAMON

International Journal of Multiphase Flow 28 (2002) 427–449

International Journal of Multiphase Flow

www.elsevier.com/locate/ijmulflow

Liquid breakup at the surface of turbulent round liquid jets in still gases

K.A. Sallam, Z. Dai [1], G.M. Faeth *

Department of Aerospace Engineering, The University of Michigan, 3000 Francois-Xavier Bagnoud Bldg., 1320 Beal Avenue, Ann Arbor, MI 48109-2140, USA

Received 5 March 2001; received in revised form 12 September 2001

Abstract

An experimental study of liquid column breakup lengths and turbulent primary breakup properties at the surface of turbulent round liquid jets in still air at standard temperature and pressure is described. Jet exit conditions were limited to non-cavitating water and ethanol flows, long length/diameter ratio (greater than 40:1) constant-diameter round injector passages, jet exit Reynolds numbers of 5000–200,000, jet exit Weber numbers of 235–270,000 and liquid/gas density ratios of 690 and 860, at conditions where direct effects of viscosity were small (e.g., liquid jet Ohnesorge numbers were smaller than 0.0053). Three liquid column breakup modes were observed, as follows: a weakly turbulent Rayleigh-like breakup mode observed at small jet exit Weber and Reynolds numbers, a turbulent breakup mode observed at moderate jet exit Weber numbers, and an aerodynamic bag/shear breakup mode observed at large jet Weber numbers. The turbulent primary liquid column breakup mode was associated with conditions where drop diameters resulting from turbulent primary breakup along the liquid surface were comparable to the diameter of the liquid column itself. The bag/shear liquid column breakup mode was observed when liquid turbulence caused large deformations of the liquid column so that portions of it were in a gaseous cross flow; this resulted in bag or shear liquid column breakup, very similar to the breakup of non-turbulent liquid jets in gaseous cross flow. Mean streamwise drop velocities after breakup were comparable to mean streamwise velocities within the jet whereas mean cross stream drop velocities after breakup were comparable to cross stream velocity fluctuations within the liquid. Rates of primary breakup at the liquid surface are reported as surface efficiency factors (the fraction of the maximum possible cross stream drop liquid flux at the surface based on the mean relative cross stream velocity of the drops at the surface and the liquid density). The resulting surface efficiency factors varied from small values near the onset of liquid surface breakup to values of the order of unity as conditions near breakup of the liquid column as a whole were approached.

* Corresponding author. Tel.: +1-734-764-7202; fax: +1-734-936-0106.
E-mail address: gmfaeth@umich.edu (G.M. Faeth).
[1] Currently with GE Aircraft Engines, Cincinnati, OH 45215, USA.

0301-9322/02/$ - see front matter
PII: S0301-9322(01)00067-2

Keywords: Atomization; Drop breakup; Sprays; Turbulence

1. Introduction

An experimental study of liquid column breakup lengths and breakup properties at the surface of turbulent round liquid jets in still air at standard temperature and pressure (STP) is described. This liquid breakup process is typical of turbulent primary breakup processes that can dominate spray formation for a variety of industrial and natural phenomena, e.g., spray atomization, liquid jets, plunge pools, bow sheets, breaking waves and waterfalls, among others (De Juhasz et al., 1932; Lee and Spenser, 1933a,b; Schweitzer, 1937; Chen and Davis, 1964; Grant and Middleman, 1966; Phinney, 1973; McCarthy and Malloy, 1974; Hoyt and Taylor, 1977a,b; Ervine and Falvey, 1987; Townson, 1988). Liquid breakup lengths of turbulent liquid jets in gases are of interest for modeling sprays because they define the region where primary breakup at the liquid surface must be considered and the start of the fully dispersed multiphase flow region. Liquid breakup properties also are of interest because they define the nature (sizes and velocities) of drops passing from the liquid phase into the dispersed phase as well as the rate at which drop liquid is produced at the boundary of the dispersed phase. Experimental methods used during this study were similar to past investigations of turbulent primary breakup by the present authors and their associates, see Wu et al. (1992, 1995), Wu and Faeth (1993, 1995), Dai et al. (1998) and Sallam et al. (1999).

Early studies of the liquid column breakup length of turbulent round liquid jets in still air include the measurements of Chen and Davis (1964), Grant and Middleman (1966), Phinney (1973) and McCarthy and Malloy (1974). Using available data, Grant and Middleman (1966) developed a correlation of mean turbulent round liquid jet breakup lengths based on dimensional analysis. Subsequently, Wu et al. (1992, 1995) and Wu and Faeth (1993, 1995) reported a more mechanistic approach for correlating the mean length of turbulent round liquid jets in still gases. This approach was based on phenomenological analysis of turbulent primary drop breakup along the liquid surface, assuming that drops were formed as a result of deformation of the liquid surface by turbulent eddies of comparable size for conditions where the eddies responsible for drop formation were in the inertial and large-eddy subranges of the turbulence spectrum (which generally is the case). This analysis showed that drop sizes progressively increased with increasing distance along the surface, in agreement, with experimental observations (Wu et al., 1992, 1995). In addition, it was also noticed that conditions satisfying the round turbulent liquid column breakup length correlation of Grant and Middleman (1966) corresponded to conditions where drops formed by turbulent primary breakup approximated the initial diameter of the liquid jet, providing a plausible physical explanation of the liquid jet breakup process (Wu et al., 1992). Subsequent evaluation of this concept was promising (Wu and Faeth, 1995), based on some preliminary measurements using present methods as well as the database used by Grant and Middleman (1966). One concern about this finding, however, was that potential aerodynamic effects that were known to affect turbulent primary breakup, due to merging of primary and

secondary breakup for some conditions (Wu and Faeth, 1993), were not resolved for liquid column breakup. A second concern was the potential effect of weakly developed turbulence where jet-exit Reynolds and Weber numbers were small (Wu et al., 1995). A final concern was that the correlation of measurements of liquid column breakup lengths for turbulent round liquid jets in still gases due to Grant and Middleman (1966) exhibited a significantly weaker dependence on jet exit Weber numbers than those anticipated from the phenomenological turbulent primary breakup theory and observed during initial measurements of turbulent liquid column breakup (Wu and Faeth, 1995).

Earlier studies of liquid breakup properties at the surface of turbulent round liquid jets in still gases include Wu et al. (1992, 1995) and Wu and Faeth (1993, 1995). These studies resolved several aspects of turbulent primary breakup at the surface of turbulent round liquid jets in still air, as follows: drop size distributions after turbulent primary breakup satisfied Simmons' universal root normal distribution, which is based on measurements of drop size distributions for a wide variety of spray conditions, and are defined completely by the Sauter mean diameter (SMD) alone, where the SMD is the diameter of a drop having the same surface area/volume ratio as the spray as a whole (cf. Simmons, 1977); drop velocities after turbulent primary breakup at a point are independent of drop size; the SMD values of drops after turbulent primary breakup progressively increase with increasing distance from the jet exit and were effectively correlated by turbulent primary breakup theory; mean streamwise and cross stream absolute drop velocities after turbulent primary breakup were associated with mean streamwise and rms fluctuating cross stream liquid velocities at the jet exit; and conditions at the onset and end of turbulent primary breakup along the liquid surface were successfully correlated using phenomenological analysis. In addition, Wu and Faeth (1995) successfully correlated mean turbulent round liquid jet breakup lengths using a turbulent primary breakup mechanism, as just discussed. Unfortunately, some important features of turbulent primary breakup of round turbulent liquid jets in still gases were not resolved during this work. First of all, the rates of drop formation due to turbulent primary breakup along the liquid surface were not found. In addition, a closely related property of drop formation rates, the cross stream drop velocity relative to the liquid surface, was not found. Finally, drop velocity information was mainly gathered for the region near the jet exit leaving substantial uncertainties about drop velocities in the critical region near the end of the liquid column. This missing information clearly is important for developing both an understanding of turbulent primary breakup and a capability to model multiphase flow involving turbulent primary breakup processes.

In view of the preceding observations, the present investigation was undertaken with the following specific objectives: to complete new measurements of the breakup lengths of turbulent round liquid jets in still gases, placing greater emphasis on conditions where small Reynolds number and aerodynamic effects were anticipated; and to complete new measurements of the rate of turbulent primary breakup along the surface of turbulent round liquid jets in still gases, seeking also to resolve the associated streamwise and cross stream drop velocities relative to the liquid surface and including conditions near the end of the liquid column. In addition, phenomenological analyses were used to interpret and correlate the new measurements, attempting to resolve both properties and the limitations of the turbulent breakup mechanism.

2. Experimental method

2.1. Apparatus

Pressure injection was used to feed the test liquids from a cylindrical storage chamber into a round nozzle directed vertically downward into still air at STP, as illustrated in Fig. 1. The storage chamber had an inside diameter and length of 165 and 305 mm, respectively. The nozzle had a smooth rounded entrance (radius of curvature equal to the nozzle passage radius) followed by round constant area passages having length-to-diameter ratios greater than 40:1 to help insure fully developed turbulent pipe flow at the jet exit for sufficiently large Reynolds numbers, as discussed by Wu et al. (1995) and references cited therein.

The test liquid was placed in the storage chamber through a port with premature outflow prevented by a cork in the nozzle exit. The liquid was forced through the nozzle, ejecting the cork at the start of liquid flow, by admitting high-pressure air to the top of the chamber through a solenoid valve. A baffle at the air inlet prevented undesirable mixing between the air and the test liquid. The high-pressure air was stored in an accumulator having a volume of 0.12 m^3 on the upstream side of the solenoid valve, with provision for accumulator air pressures up to 1900 kPa. The test liquid was captured in a baffled tub. The nozzle assembly could be traversed vertically with an accuracy of 0.5 mm using a linear bearing system in order to accommodate rigidly mounted optical instrumentation.

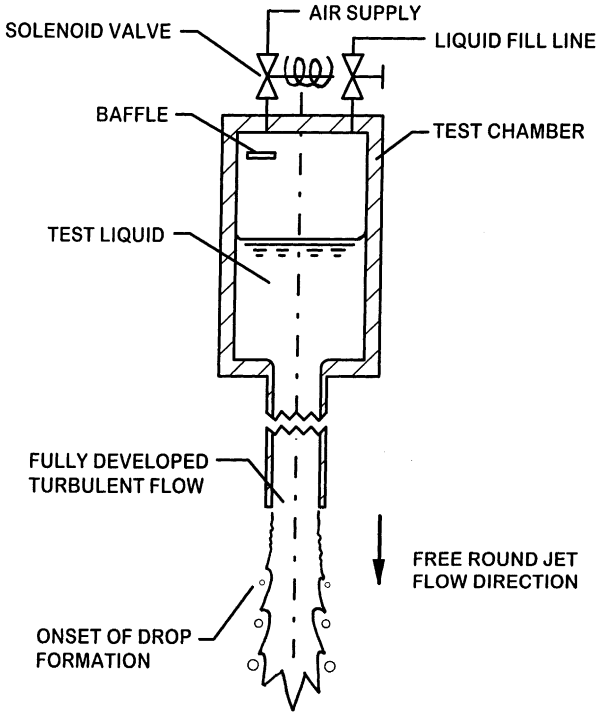

Fig. 1. Sketch of the turbulent round liquid jet apparatus.

Liquid injection times of 100–400 ms were long compared to flow development times of 6–70 ms. Present optical measurements required less than 0.1 ms for triggering and data acquisition which did not impose any limitation on flow times. Liquid jet velocities were calibrated as a function of the nozzle pressure drop by the measuring liquid surface velocities using double-pulse shadowgraphs as discussed later.

2.2. Instrumentation

Instrumentation consisted of single- and double-pulse shadowgraphy and holography using an arrangement similar to Dai et al. (1998). The light sources for both systems were two frequency-doubled YAG lasers (Spectra Physics Model GCR-130, 532 nm wavelength, 7 ns pulse duration, and up to 300 mJ per pulse) that could be controlled to provide pulse separations as small as 100 ns (pulse separations were measured with a digital oscilloscope).

Pulsed shadowgraphy was used to find mean liquid column breakup lengths, mean streamwise drop and liquid surface velocities, mean cross stream absolute drop velocities and mean cross stream drop velocities relative to the liquid surface. The laser beams were expanded to provide beams with diameters up to 30 mm that passed through the region being observed. The shadowgraphs were recorded using a 100 mm $\times$ 125 mm film format at magnifications up to 7:1, with the camera focused at the median plane of the liquid jet. These photographs were obtained with an open camera shutter under darkroom conditions so that the laser pulse durations controlled the exposure time and were short enough to stop liquid surface and drop motion. The use of different pulse strengths allowed directional ambiguity to be resolved. Data were obtained from the photographs by mounting them on a computer controlled x–y traversing system (having a 1 μm resolution) and observing the images with an MTI model 65 video camera.

Several pulsed shadowgraph images were averaged in order to find mean liquid column breakup lengths with experimental uncertainties (95% confidence) less than 10%. Measurements of liquid surface velocities were based on the motion of particular points identifiable by surface irregularities, summing over 40–200 such points to find streamwise surface velocities with experimental uncertainties (95% confidence) less than 5%. Measurements of mean streamwise and cross stream drop velocities were based on the motion of the centroid of the drops. Finding these averages was simplified because drop velocity distributions were essentially uniform, as noted earlier. The experimental streamwise and cross stream velocities summed over 40–240 drops were used to find mass-averaged mean absolute streamwise and cross stream velocities. The experimental uncertainties (95% confidence) were smaller than 5% and 20%, for the streamwise and cross stream velocities, respectively. Finally, mean-averaged cross stream drop velocities relative to the liquid surface were found by summing the relative cross stream velocities of 40–400 drops with experimental uncertainties (95% confidence) smaller than 20%. In all cases, experimental uncertainties were dominated by sampling limitations.

Single-pulse holography was used to find drop liquid fluxes at the liquid surface due to turbulent primary breakup. This was done by measuring the volume of drop liquid within an annular segment defined by the angle between two alignment pins (positioned outside the spray-containing region) and the axis of the liquid jet, with the distance above the mean position of the liquid surface given by the distance the drops move at the mean relative velocity with respect to the liquid surface for a preselected sampling time (chosen to avoid the excessive shot noise that is

present when the number of drops in the annular segment becomes too small, and to avoid effects of drop relaxation in the dispersed flow region when the thickness of the annular segment becomes too large). Fortunately, for the conditions that were considered, selection of sampling times over relatively broad ranges yielded essentially the same results as long as the number of sample realizations considered was sufficiently large.

An off-axis holographic arrangement was used for the drop liquid flux measurements. The optical penetration properties of the holograms were improved by reducing the diameter of the object beam through the flow by roughly a factor of 3 and subsequently expanding the beam back to the size of the 100 mm diameter reference beam when the two beams were optically mixed to create the hologram. The arrangement allowed drops as small as 5 μm diameter to be seen and drops as small as 10 μm diameter to be measured with 10% accuracy. The holograms were reconstructed using a 35 mW HeNe laser, with the laser beam collimated at a 50 mm diameter and passed through the hologram to provide a real image of the spray. Analysis of the hologram images was the same as the shadowgraphs except the x–y traversing of the holograms was supplemented by z traversing (with 5 μm resolution) of the video camera to allow for the three-dimensional nature of the hologram reconstruction.

Methods of data reduction of the holograms were the same as Wu et al. (1992) and Wu and Faeth (1993, 1995). Irregular drops were assumed to be ellipsoids and their volumes were found from the measured major and minor diameters of the ellipsoid. The reconstruction traversing system defined the volume of the annular segment sampling volume based on the known positions of the two alignment pins, the center of the liquid column and the distance calibrations of the traversing system. Adjusting the angle of the segment dealt with occasional problematical configurations where a large drop near the angular boundary of the sample segment required excessive depth of field resolution to find the cross stream liquid drop flux. Experimental uncertainties of liquid flux measurements due to the definition of irregular objects as ellipsoids are difficult to quantify; otherwise, 40–60 sample volumes were evaluated to yield mean radial liquid

Table 1
Summary of test conditions[a]

Parameter	Range
Liquid	Water[b], ethanol[c]
Initial jet diameter (d)	1.9, 4.8 and 8.0 mm
Jet exit mean liquid velocity (u_0)	3–40 m/s
Liquid/gas density ratio (ρ_L/ρ_G)	860 (water), 690 (ethanol)
Jet exit Reynolds number ($Re = \rho_L u_0 d/\mu_L$)	5000–200,000
Jet exit Weber number ($We = \rho_L u_0^2 d/\sigma$)	235–270,000
Jet exit Ohnesorge number ($Oh = \mu_L/(\rho_L d\sigma)^{1/2}$)	0.0015–0.0053
Normalized liquid jet length (L_c/d)	50–300

[a] Round turbulent liquid jets injected from long length-to-diameter ratio (greater than 40) passages having smooth entries into still air at standard temperature and pressure (STP), i.e., 98.7 kPa and 294 ± 2 K. Properties of air taken as follows: density = 1.17 kg/m^3 and absolute viscosity = 18.5×10^{-4} kg/ms.

[b] Properties of water taken at standard temperature and pressure as follows: density = 997 kg/m^3, absolute viscosity 8.94×10^{-4} kg/ms and surface tension = 70.8 mN/m.

[c] Properties of ethanol taken at standard temperature and pressure as follows: density = 800 kg/m^3, absolute viscosity = 16.0×10^{-4} kg/ms and surface tension = 24.0 mN/m.

drop fluxes with experimental uncertainties (95% confidence) less than 30%, mainly dominated by sampling limitations.

2.3. Test conditions

Present test conditions are summarized in Table 1. The test liquids were water and ethanol with jet exit diameters of $d = 1.9$, 4.8 and 8.0 mm, and jet exit velocities of $u_0 = 3$–40 m/s. Denoting liquid and gas properties with the subscripts L and G, the liquid/gas density ratios were $\rho_L/\rho_G = 860$ and 690 for water and ethanol, respectively. Other physical properties, e.g., $\mu =$ absolute viscosity and $\sigma =$ surface tension, are summarized in Table 1 for air, water and ethanol.

The jet exit dimensionless parameters, defined in Table 1, are as follows: Reynolds numbers, $Re = 5000$–200,000; Weber numbers, $We = 235$–270,000; and Ohnesorge numbers, $Oh = 0.0015$–0.0053. These conditions yielded mean normalized liquid jet breakup lengths, $L_c/d = 50$–300. The jet exit Reynolds number range implies that present results were dominated by effects of turbulent primary breakup but limiting behavior at small Reynolds numbers was still probed.

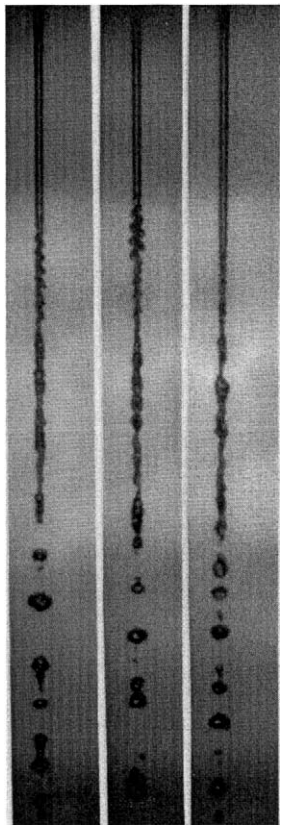

Fig. 2. Pulsed shadowgraphs of Rayleigh-like breakup of weakly turbulent round liquid jets at a small Weber number: water jets in still air, $d = 1.9$ mm, $Re = 5030$ and $We = 235$.

The small jet exit Ohnesorge numbers imply that direct effects of liquid viscosity on liquid breakup were small, see Hsiang and Faeth (1992, 1995) and Faeth (1996) and references cited therein. Present measurements were supplemented by the earlier results of Chen and Davis (1964), Grant and Middleman (1966) and Wu and Faeth (1995). Original sources should be consulted for information about the test conditions used during the earlier studies, however, they generally involved jet exit Reynolds, Weber and Ohnesorge numbers similar to the present experiments.

3. Results and discussion

3.1. Weakly turbulent liquid column breakup

Three modes of liquid column breakup were observed for turbulent round liquid jets injected into still air at STP, as follows: a weakly turbulent Rayleigh-like breakup mode observed at small jet exit Weber and Reynolds numbers, a turbulent breakup mode observed at moderate jet exit Weber and Reynolds numbers, and an aerodynamic bag/shear breakup mode observed at large jet exit Weber numbers. Flow visualization and phenomenological analysis to develop breakup length correlations will be considered for each of these mechanisms in the following, beginning with weakly turbulent Rayleigh-like liquid column breakup in this section.

Three examples of the appearance of the turbulent round liquid jet breakup process at small We and Re are illustrated in Fig. 2. These results were obtained for $We = 235$ and $Re = 5030$, where the turbulence at the jet exit is only weakly developed. For such conditions, the liquid column is not significantly distorted by the turbulence, distortion of the liquid column is generally axisymmetric, and breakup involves Rayleigh-like breakup of a liquid column that is distorted in a regular way. This yields a stream of drops having a relatively limited number of diameters with the largest drops having diameters roughly twice the diameter of the original liquid column, which is characteristic of Rayleigh-like liquid column breakup in still gases (Weber, 1931).

A simple analysis can provide some insight into the weakly turbulent breakup process and help to suggest a convenient way of correlating these breakup lengths. To do this, assume that aerodynamic effects are small, that effects of liquid viscosity are also small (which is the case for all results considered here due to the small Ohnesorge numbers of the experimental liquid jets), and that breakup of the liquid column occurs when the amplitudes of liquid surface disturbances present at the jet exit grow to the point where they reach the liquid jet axis. Based on the analysis of Rayleigh breakup for these conditions, a simple correlation for the breakup length is obtained, as follows (Weber, 1931):

$$L_c/d = C_r\, We^{1/2}, \tag{1}$$

where C_r is an empirical parameter having a magnitude of the order of unity. Eq. (1) follows from classical analysis to find the time required for the Rayleigh breakup, t_r, assuming that the velocity of the flow in the liquid jet remains constant at u_0. The length required for Rayleigh breakup then becomes $L_c = u_0 t_r$, which yields Eq. (1) upon substituting the classical expression for the Rayleigh breakup time (or capillary time scale) for t_r (Weber, 1931). The value of C_r is known to be a function of disturbance levels of the liquid column at the jet exit (Weber, 1931); therefore, it is

likely to be affected by jet exit turbulence properties for conditions representative of the weakly turbulent breakup process.

3.2. Turbulent liquid column breakup

Three examples of the appearance of the turbulent round liquid jet breakup process observed at moderate *We* and *Re* are illustrated in Fig. 3. These results were obtained for $We = 1670$ and $Re = 13{,}690$ where the liquid turbulence at the jet exit is reasonably well developed. This condition yields a liquid jet whose surface becomes distorted in the cross stream direction by turbulence; the distortion is irregular (i.e., not axisymmetric); and the liquid jet breakup process is associated with liquid disturbances having characteristic dimensions comparable to the diameter of the liquid jet itself. This yields drops having a broad distribution of sizes with little tendency for a limited number of groups of nearly monodisperse drops. Thus, liquid jet breakup at these conditions appears to involve the turbulent primary breakup mechanism proposed by Wu et al. (1992, 1995). As noted earlier, definition of this mechanism followed from the observation that the estimates of drop diameters after turbulent primary breakup due to Wu et al. (1992, 1995) showed that the

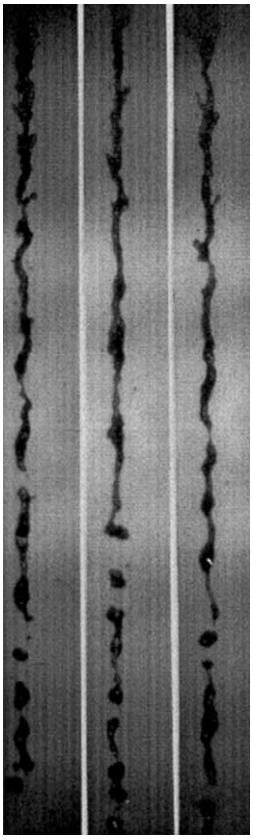

Fig. 3. Pulsed shadowgraphs of turbulent round liquid jet breakup at a moderate Weber number: water jet in still air, $d = 1.9$ mm, $Re = 13{,}690$ and $We = 1670$.

SMD of drops after turbulent primary breakup were approximately the same as the initial jet diameter for conditions corresponding to the turbulent round liquid jet breakup length estimated from the Grant and Middleman (1966) correlation. The corresponding liquid jet breakup length expression can be obtained from the correlation for the SMD after turbulent primary breakup given by the phenomenological analysis of Wu et al. (1992), as follows:

$$\mathrm{SMD}/\Lambda = C_{sx}(x/(\Lambda\, We_{\Lambda}^{1/2}))^{2/3}, \tag{2}$$

where Λ is the cross stream (radial) integral length scale at the jet exit, the empirical parameter $C_{sx} = 0.65$ based on the measurements of Wu et al. (1992), x is the streamwise distance from the jet exit, and $We_{\Lambda} = \rho_{\mathrm{L}}\Lambda u_0^2/\sigma$ is the Weber number based on the jet exit cross stream (radial) integral length scale. Then, assuming that $\mathrm{SMD} \sim d$ at the liquid jet breakup condition where $x = L_{\mathrm{c}}$, Eq. (2) yields the following expression for the normalized liquid breakup length (Wu and Faeth, 1995):

$$L_{\mathrm{c}}/d = C_{\mathrm{c}}\, We^{1/2}, \tag{3}$$

where C_{c} is an empirical parameter expected to have a magnitude of the order of unity and the fact that $\Lambda \sim d$ for fully developed turbulent pipe flow has been exploited.

The corresponding turbulent round liquid jet breakup length correlations developed by Grant and Middleman (1966), based on both their measurements and those of Chen and Davis (1964), is as follows:

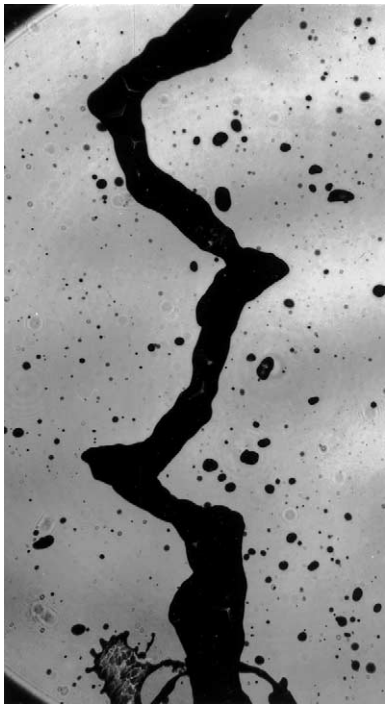

Fig. 4. Pulsed shadowgraph of large cross stream distortions near the tip of a turbulent round liquid jet at a large Weber number: water jet in still air, $d = 4.8$ mm, $Re = 97{,}100$, $We = 33{,}100$ at a distance of 1040 mm from the jet exit.

$$L_c/d = 8.51\ We^{0.32}. \quad (4)$$

The noticeable reduction of the power of the Weber number between the correlation of Eq. (3) based on turbulent primary breakup concepts and Eq. (4) based on direct correlation of measurements using dimensional analysis is evident, as noted earlier. The difference comes about because Eq. (4) involves measurements that extend over several specific breakup regimes, whereas Eq. (3) involves a more mechanistic way of treating one of the specific breakup regimes (i.e., the turbulent liquid column breakup regime). Thus, Eq. (3) was explored as a way of correlating liquid column breakup lengths for turbulent liquid column breakup conditions.

3.3. Turbulent bag/shear liquid column breakup

When values of *We* significantly exceeded the upper end of the range of measurements considered by Chen and Davis (1964) and Grant and Middleman (1966), the turbulent liquid column breakup mechanism changed. At these conditions, the turbulence distorts the liquid jet to a much greater degree that the jet diameter, leading to an aerodynamic turbulent liquid column breakup mechanism of the liquid jet as a whole. Note that this occurs in the turbulent bag/shear liquid column break regime even though earlier studies of Hoyt and Taylor (1977a,b) and Wu and Faeth (1993) show that aerodynamic effects at the liquid/gas interface do not have a significant influence

Fig. 5. Pulsed shadowgraph of bag-like breakup of large cross stream distortions near the tip of a turbulent round liquid jet at a large Weber number: water jet in still air, $d = 4.8$ mm, $Re = 97{,}100$ and $We = 33{,}100$ at a distance of 1040 mm from the jet exit.

on liquid-phase velocities and turbulence properties prior to breakup, i.e., aerodynamic effects only become significant when the liquid column is in cross flow.

Fig. 4 is a pulsed shadowgraph photograph of the large-scale distortion of the liquid jet just prior to aerodynamic turbulent round liquid jet breakup. Typical of the general behavior of turbulent primary breakup, the small-scale liquid surface distortions due to small-scale eddies seen nearer to the jet exit (see the shadowgraph photographs of Wu et al., 1992) are absent because the small-scale eddies have decayed. Thus, all that remain are large-scale distortions of a nearly non-turbulent liquid column. This places most liquid column elements in cross flow which leads to modes of breakup similar to those observed during breakup of non-turbulent round liquid jets in gaseous cross flows, e.g., see the observations of Wu et al. (1997) and Mazallon et al. (1999). Two types of breakup of the liquid jet in cross flow were observed that were also observed for non-turbulent round liquid jets in cross flow (Mazallon et al., 1999) as follows: (1) bag-type liquid jet breakup, which involves the formation of bag-like structures in the liquid jet and their subsequent breakup into drops (similar to secondary drop breakup in the bag-breakup regime, see Chou et al., 1998 and references cited therein) illustrated in Fig. 5; and (2) shear-type liquid jet breakup, which involves the formation of ligaments along the sides of the liquid jet and their subsequent breakup into drops (similar to secondary drop breakup in the shear-breakup regime, see Chou and Faeth, 1998 and references cited therein) illustrated in Fig. 6. Recognizing the potential

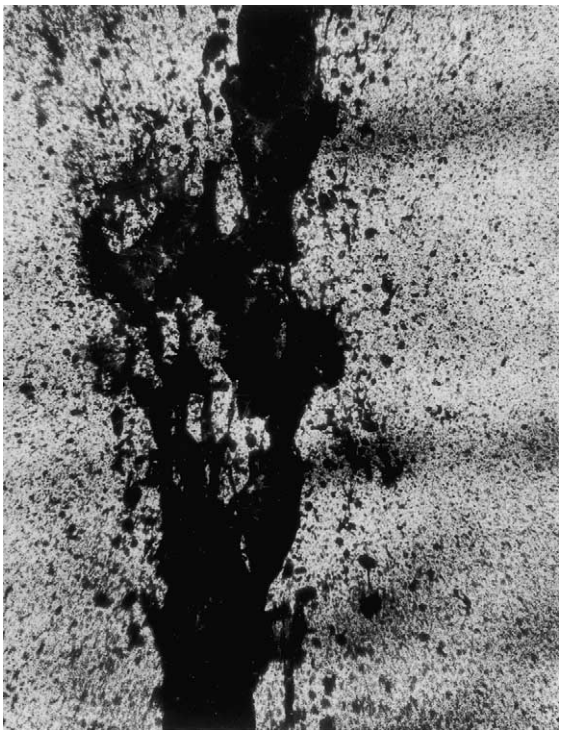

Fig. 6. Pulsed shadowgraph of shear-like breakup near the tip of a turbulent round liquid jet at a large Weber number: water jet in still air, $d = 4.8$ mm, $Re = 129{,}000$ and $We = 271{,}000$ at a distance of 1300 mm from the jet exit.

presence of these two modes of breakup, as well as combinations of them at intermediate conditions (similar to the breakup of drops in the multimode-breakup regime, see Dai and Faeth, 2001 and references cited therein), this process will be termed bag/shear breakup in the following. Recalling that these modes of liquid jet breakup were observed by Mazallon et al. (1999) for non-turbulent liquid jet breakup in cross flowing gases; these mechanisms are clearly associated with aerodynamic effects.

A simplified phenomenological analysis can provide some insight into the bag/shear breakup process and a convenient way of correlating these breakup lengths. First of all, by analogy to the secondary breakup of drops, the time required for bag, multimode or shear breakup of the liquid column, t_b, is given by (Mazallon et al., 1999)

$$t_b = C_b(\rho_L/\rho_G)^{1/2} d/u_0, \tag{5}$$

where C_b is an empirical parameter of the order of unity. Based on past findings for secondary drop breakup, the value of C_b is not expected to differ very much with changes of the specified

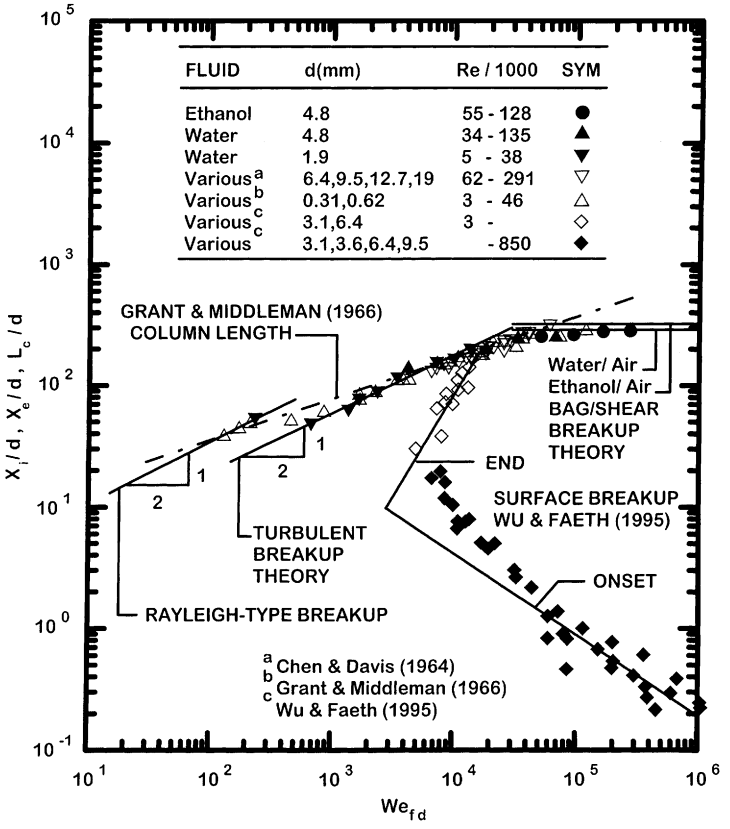

Fig. 7. Mean liquid column breakup lengths of turbulent round liquid jets in still air plotted according to the weakly turbulent, turbulent and bag/shear liquid column breakup analyses: measurements of Chen and Davis (1964), Grant and Middleman (1966) and the present investigation. Also, onset and end of liquid surface breakup of turbulent round liquid jets in still air plotted according to the measurements and predictions of Wu and Faeth (1995).

breakup mode, e.g., bag, multimode or shear breakup, or with the value of *We* of the breakup process (Hsiang and Faeth, 1992; Dai and Faeth, 2001). Now assume that the point of breakup corresponds to the streamwise distance reached by the column while moving at the mean jet exit velocity for a time, t_b, as follows:

$$L_c = u_0 t_b. \tag{6}$$

Combining Eqs. (5) and (6) then yields an expression for the aerodynamic bag/shear breakup length, as follows:

$$L_c/d = C_b(\rho_L/\rho_G)^{1/2}, \tag{7}$$

where the flow leaving the jet exit must be turbulent. This result, combined with the properties of turbulent primary breakup (Wu et al., 1992; Wu and Faeth, 1993, 1995), suggests that for large enough *Re* and *We* to yield turbulent jet exit conditions, L_c/d first increases with *We* according to Eq. (3) and then becomes independent of *We* at large values of this parameter at conditions specifically governed by ρ_L/ρ_G.

The liquid jet breakup length correlation of Eq. (7) is identical in form to early correlations of liquid jet breakup lengths during pressure atomization processes measured at large pressures by Hiroyasu et al. (1982) and Chehroudi et al. (1985). Their test conditions, however, imply relatively small values of L_c/d where distortion of the entire liquid column in the manner illustrated in Figs. 4–6 is improbable. Instead, the high-pressure aerodynamic mechanism is much more likely to involve merging of turbulent primary breakup and secondary breakup of ligaments protruding from the liquid surface, as discussed by Wu and Faeth (1993). This mechanism only appears for pressures somewhat larger than atmospheric pressure for liquid injection into still gases (Wu and Faeth, 1993), however, and is not a factor during the present investigation.

3.4. Mean liquid column breakup lengths

In order to assess ideas about the weakly turbulent, the turbulent and the bag/shear liquid column breakup process, present and past measurements of L_c/d are plotted as a function of *We* in Fig. 7. Measurements of values of L_c/d on this plot include those from Chen and Davis (1964), Grant and Middleman (1966) and the present investigation, the latter superseding earlier measurements of L_c/d in this laboratory due to Wu et al. (1995). Several correlations of the measurements are also shown in the plot, as follows: (1) the correlation of the weakly turbulent (Rayleigh) breakup regime based on Eq. (1) which has been fitted to present measurements in the weakly turbulent breakup regime to yield the best-fit correlation:

$$L_c/d = 5.0\, We^{1/2} \tag{8}$$

for $We < 400$ with a standard deviation of C_r of 0.5 based on present measurements; (2) the correlation due to Grant and Middleman (1966) based on the measurements of Chen and Davis (1964) and Grant and Middleman (1966) for *We* of 100–10,000; (3) the best-fit correlation of turbulent breakup theory based on Eq. (3)

$$L_c/d = 2.1\, We^{1/2}, \tag{9}$$

where the standard deviation of the coefficient, C_c, is 0.2, based on present measurements for *We* of 670–13,700; and (4) the best-fit correlation of bag/shear breakup of liquid ethanol in air based on Eq. (7), as follows:

$$L_c/d = 11.0(\rho_L/\rho_G)^{1/2}, \tag{10}$$

where the standard deviation of the coefficient, C_b, is 0.3 based on present measurements for $We > 30{,}000$. Another correlation illustrated in the plot is for bag/shear breakup of water jets in still air computed from Eq. (10). The effect of the slightly different density ratios for injection of ethanol and water into air at standard temperature and pressure, however, is seen to be modest compared to present experimental uncertainties.

Present measurements, those of Chen and Davis (1964), and those of Grant and Middleman (1966), are in good agreement for the range of conditions where they can be compared. The Grant and Middleman (1966) expression for L_c/d given by Eq. (4) is also seen to provide a good correlation of the measurements over the range of *We* that they considered. Closer examination reveals, however, that this performance may be an artifact of the transition to different breakup mechanisms at the small and large *We* ranges of measurements, helping to explain the reduced power of *We* in their breakup length correlation, Eq. (4), compared to the expected power of *We* for turbulent primary breakup given by Eq. (3). For example, at small *We*, jet Reynolds numbers become small, approaching values of 2000 so that effects of weakly developed turbulence become a factor; this observation is supported by transitional-like behavior where the measurements shift from the Grant and Middleman (1966) correlation for *We* smaller than 400 to the present turbulent breakup correlation for *We* larger than 800 (the corresponding transitional range of *Re* is 3000–12,000 which is supportive of the effects of weakly developed turbulence, see Wu et al., 1995 and references cited therein). This behavior is also supported by the Rayleigh-like breakup appearance of the liquid columns for the small *We* number conditions in Fig. 7, e.g., the breakup visualizations at small *We* illustrated in Fig. 2. Finally, the trend that L_c/d at small *We* generally agrees with the anticipated behavior of Rayleigh-like breakup provided by Eq. (1) also supports transition between Rayleigh-like and turbulent liquid column breakup for the small *We* range of conditions illustrated in Fig. 7. Liquid column breakup at small Reynolds numbers, however, depends on liquid passage disturbances that are difficult to control (Weber, 1931; Sallam et al., 1999). The present liquid injection system was not designed with potential application to Rayleigh breakup in mind, however, and further consideration of laminar jet exit conditions, beyond identifying the potential small Reynolds number limit of turbulent liquid column breakup, was beyond the scope of the present investigation.

At large *We*, L_c/d proved to be relatively independent of *We* as suggested by Eqs. (7) and (10) for an extended range of values of *We* of 30,000–300,000 in agreement with the bag/shear breakup mechanism (as noted earlier, the variation of liquid/gas density ratio over the present test range does not have a significant influence on liquid column breakup lengths compared to experimental uncertainties). This behavior also tends to reduce the slope of the apparent variation of L_c/d with *We* for the range of conditions considered by Grant and Middleman (1966). With these effects noted, the intermediate *We* region in the range 600–30,000 is seen to be in reasonably good agreement with behavior expected for the turbulent liquid column breakup mechanism from Eqs. (3) and (9). Finally, the various correlations all seem to be reasonable, with C_r in Eq. (1) and C_c in Eq. (3) of the order of unity as expected, and C_b in Eq. (7) comparable to earlier measurements of

aerodynamic liquid column breakup due to Hiroyasu et al. (1982) and Chehroudi et al. (1985). In addition, the best-fit correlation of the turbulent liquid column breakup mechanism also properly indicates liquid column breakup when sizes resulting from turbulent primary breakup are comparable to the initial liquid jet diameter; this behavior can be confirmed from the correspondence between the Grant and Middleman (1966) results for both turbulent primary breakup in Wu et al. (1992) and for the liquid jet breakup lengths in Fig. 7.

Before turning to the consideration of drop velocities after turbulent primary breakup, and rates of turbulent primary breakup, more information about the range of conditions where turbulent primary breakup occurs at STP will be discussed, considering results reported by Wu and Faeth (1995). This includes conditions for the onset and end of turbulent primary breakup along the liquid surface that are also illustrated in Fig. 7. Conditions for the onset of turbulent primary breakup along the liquid surface could be correlated as the condition where the kinetic

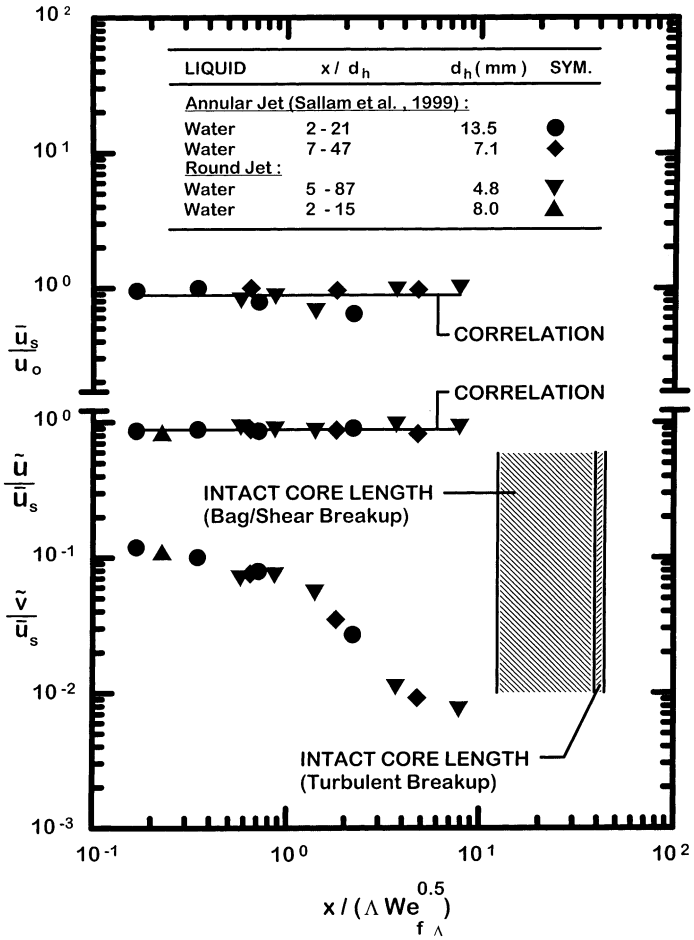

Fig. 8. Mean surface streamwise velocities, and absolute mean streamwise and cross stream drop velocities, as a function of streamwise distance from the jet exit.

energy of eddies of particular size was sufficient to provide the surface tension energy of drops of comparable size; all conditions of this nature were found to correspond to turbulent eddies in the inertial range of turbulence during the turbulent primary breakup study of Wu and Faeth (1995). A second condition was found where turbulent primary breakup ended along the surface of turbulent round liquid jets in still gases; this condition was reached in the large-eddy subrange of the turbulence spectrum where the kinetic energy of eddies of particular size once again was comparable to the surface tension energy of drops of comparable size. Thus, the region of turbulent primary breakup along the surface of turbulent round liquid jets in still gases at STP is confined by conditions for the onset of turbulent primary breakup, for the end of turbulent primary breakup, for the end of the liquid column due to turbulent breakup, and for the end of the liquid column due to aerodynamic bag/shear breakup. The velocity properties of drops after turbulent primary breakup, and the rate of liquid breakup within this region, will be considered next.

3.5. Drop velocities after turbulent primary breakup

Similar to earlier findings for drop velocity distributions after turbulent primary breakup of round and plane liquid jets in still gases and plane liquid wall jets in still gases (Wu et al., 1992; Wu and Faeth, 1993; Dai et al., 1998; Sallam et al., 1999), drop velocity distributions after turbulent primary breakup were essentially uniform. Thus, drop velocities will be reported as mass-averaged absolute streamwise velocities, $\tilde{u}$, and as mass-averaged absolute and relative (with respect to the liquid surface) cross stream (radial) velocities, $\tilde{v}$ and $\tilde{v}_r$, in order to simplify presentation of the measurements.

Measured mean streamwise and cross stream absolute velocities associated with turbulent primary breakup of turbulent liquids in still gases are illustrated in Fig. 8. Measured velocities shown in the figure include time-averaged local streamwise liquid surface velocities normalized by the jet exit mean velocity, $\bar{u}_s/u_0$, and the mass-averaged mean streamwise and cross stream absolute velocities of the drops after turbulent primary breakup normalized by the local time-averaged streamwise liquid surface velocity, $\tilde{u}/\bar{u}_s$ and $\tilde{v}/\bar{u}_s$. These results are plotted in terms of the streamwise variable that provides correlations of the SMD of drops after turbulent primary breakup of round and plane turbulent liquid jets in still gases, e.g., $x/(\Lambda\, We^{0.5})$. Also shown in the figure are the downstream limits of the liquid column lengths for both turbulent and bag/shear breakup (note that the latter appears as a band because it is not correlated specifically in terms of $x/(\Lambda\, We^{0.5})$). Two sets of measurements are shown in the figure for the various velocities: the measurements for nearly plane (annular) jets due to Sallam et al. (1999) and the present measurements for round jets. Hydraulic diameters, d_h, are noted in Fig. 8 for both the round and plane jets; naturally, the hydraulic diameter and the actual diameter are the same for the round jets.

The results plotted in Fig. 8 show first of all that the normalized measurements for round and plane turbulent liquid jets are essentially the same. Next, $\bar{u}_s/u_0$, is nearly independent of streamwise distance over the length of the liquid column for a round jet or the length of the liquid sheet for a plane jet, or

$$\bar{u}_s/u_0 = 0.89 \tag{11}$$

with a standard deviation of the ratio of 0.04 over the entire database illustrated in Fig. 8. Similarly, the mean streamwise drop velocity is closely associated with the local streamwise liquid surface velocity, with all the measurements illustrated in Fig. 8 yielding

$$\tilde{u}/\bar{u}_s = 0.88 \tag{12}$$

with a standard deviation of this ratio of 0.03, over the length of the liquid column. Mass-averaged cross stream velocities, however, behave rather differently from streamwise velocities in that they decrease with increasing streamwise distance. Earlier considerations also showed that mass-averaged absolute cross stream velocities for round and plane liquid free jets in still gases were not in good agreement with measurements of these velocities for plane turbulent liquid wall jets in still gases (Sallam et al., 1999). The variation of $\tilde{v}$ with streamwise distance for round and plane turbulent liquid free turbulent jets, however, is quite plausible. In particular, $\tilde{v}/\bar{u}_s = 0.037$ near the jet exit for wall jets, as will be shown shortly. Thus, near the jet exit, $\tilde{v}/\bar{u}_s$ for free jets is larger than for wall jets because cross stream flapping of the liquid core is not constrained by the wall for free jets. In contrast, as the end of the liquid column is approached for free jets, the mean cross stream velocity should become small due to symmetry, i.e., cross stream motion in either direction is equally probable when the end of the liquid column is reached. The presence of the

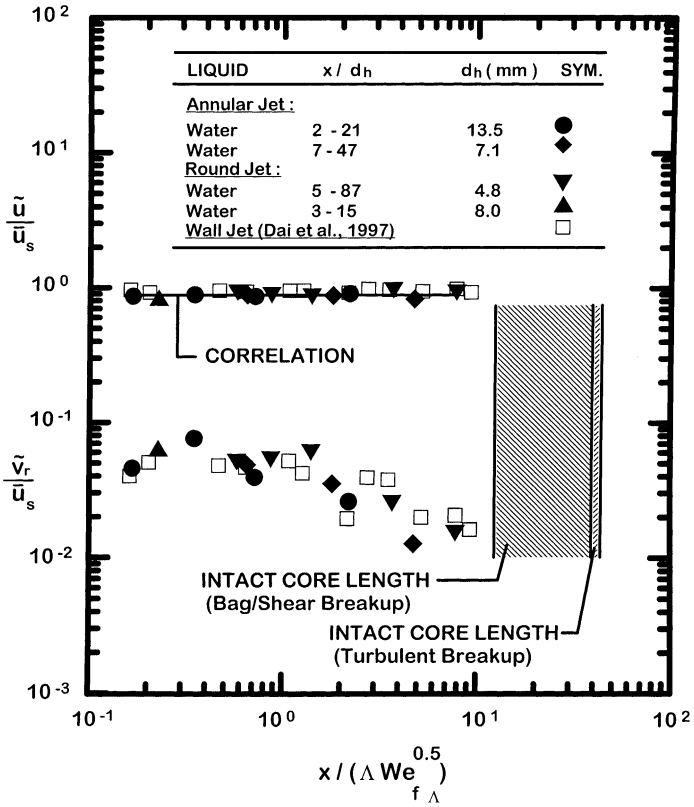

Fig. 9. Absolute mean streamwise and relative cross stream drop velocities as a function of streamwise distance from the jet exit.

wall, however, constrains cross stream motion so that $\tilde{v}/u_s$ tends to remain larger for wall jets than for free jets near the end of the liquid sheet (or column).

The previous discussion comparing the behavior of cross stream mass-averaged velocities of drops after turbulent primary breakup for liquid free jets and wall jets is further clarified by considering the relative cross stream velocities illustrated in Fig. 9. Independent variables and the liquid column limits are the same in Fig. 9 as in Fig. 8, except that results for plane wall jets from Dai et al. (1998) are shown along with the results for plane and round free jets. Adding the wall jet data to the free jet results has little effect on the correlation of $\tilde{u}/\bar{u}_s$ which is adequately expressed by Eq. (11) for all three flows. This finding also suggests very little modification of the streamwise velocity of liquid drops during the breakup process of the liquid surface. In addition, the relative cross steam velocities for all three flows exhibit essentially the same streamwise variation,

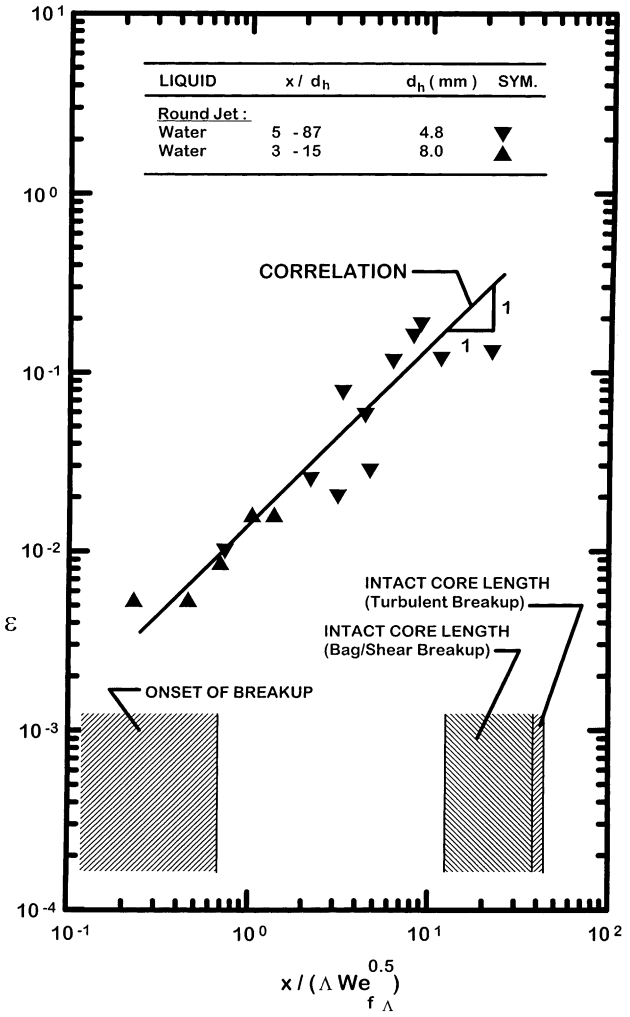

Fig. 10. Mean surface efficiency factors as a function of streamwise distance from the jet exit.

suggesting that the increased variation of $\tilde{v}/\bar{u}_s$ for the free jets seen in Fig. 8 can be attributed to flapping of the liquid jet as a whole. Finally, $\tilde{v}_r/\bar{u}_s$ near the jet exit takes on values of 0.04–0.05 which are comparable to cross stream rms velocity fluctuations not too near the wall for fully developed turbulent pipe flow (Tennekes and Lumley, 1972) as might be expected for conditions where surface tension forces at the liquid surface are rather small compared to the momentum of eddy sizes responsible for the creation of drops by turbulent primary breakup.

3.6. Liquid breakup rates due to turbulent primary breakup

The last liquid surface property that was studied during the present investigation was the flux of liquid drops relative to the liquid surface as a result of turbulent primary breakup along the liquid surface, or $\dot{m}''_L$. In order to normalize this variable, it was defined in terms of the liquid surface breakup efficiency factor, ε, as follows:

$$\varepsilon = \dot{m}''_L/(\rho_L \tilde{v}_r), \tag{13}$$

where the limit $\varepsilon = 1$ represents conditions where liquid drops are forming in a continuous manner over all the projected surface area of the liquid surface. The actual appearance of turbulent primary breakup, as the result of the Rayleigh-breakup of the tips of growing ligaments along the surface, see the pulsed shadowgraph images of turbulent breakup processes appearing in Wu et al. (1992), Wu and Faeth (1993), Dai et al. (1998) and Sallam et al. (1999), however, suggests that generally $\varepsilon < 1$, if not $\ll 1$.

Present measurements of ε for turbulent primary breakup of turbulent round liquid jets in still air are illustrated in Fig. 10. Similar to Figs. 8 and 9, the independent variable in this figure is taken to be $x/(\Lambda\, We^{0.5})$ which is the characteristic streamwise variable used to correlate the SMD after turbulent primary breakup and the liquid column breakup length. Limits giving the onset of turbulent primary breakup as well as the liquid column length are shown in the plot to help define the region of the liquid column where turbulent primary breakup was occurring. The streamwise independent variable used in Fig. 10 is only a suitable correlating variable for turbulent breakup of the liquid column; therefore, other criteria for the onset and end of turbulent primary breakup appear as bands in Fig. 10.

The correlation of the present measurements yields a simple empirical power law relationship for ε over the present test range, as follows:

$$\varepsilon = 0.012[x/(\Lambda\, We^{0.5})], \tag{14}$$

where actual best-fit power of the independent variable of Eq. (14) is 0.9 with an experimental uncertainty (95% confidence) of 0.2 which is not statistically different from unity; therefore, the simple form has been retained for the present data correlation. The experimental uncertainty (95% confidence) of the coefficient is 0.006 and the correlation coefficient of fit is 0.92, which is good. Moreover, the trend of the measurements in Fig. 10 appears to be quite reasonable. Based on its definition, small values of ε, approaching 0, are expected near the onset of breakup. On the other hand, as the end of the liquid column is approached, large liquid breakup efficiencies are expected. Thus, the values of ε in the range 0.1–0.3 at the downstream end of the range of measurements illustrated in Fig. 10 are quite reasonable.

4. Conclusions

This investigation involved measurements of liquid column breakup lengths and turbulent primary breakup properties at the surface of turbulent round liquid jets in still air at STP. Jet exit conditions were limited to non-cavitating water and ethanol flows from large length/diameter ratio constant cross sectional area injector passages having smooth entries and jet exit Reynolds numbers of 5000–200,000, jet exit Weber numbers of 235–270,000 and liquid/gas density ratios of 690 and 860, at conditions where direct effects of liquid viscosity were small. The major conclusions of the study are as follows:

1. Three liquid column breakup modes were observed, as follows: a weakly turbulent Rayleigh-like breakup mode for $We < 300$ and $Re < 5000$; where liquid column breakup lengths could be correlated according to Eq. (8); a turbulent breakup mode for $600 < We < 30{,}000$ where liquid column breakup lengths could be correlated according to Eq. (9) and breakup follows when drop diameters resulting from turbulent primary breakup become comparable to the diameter of the liquid column itself; and an aerodynamic bag/shear breakup mode for $We > 30{,}000$ where liquid column breakup lengths could be correlated according to Eq. (10) and breakup occurs when small-scale turbulence has disappeared and the liquid column is distorted in the cross stream direction by large-scale turbulence so that breakup occurs by bag- and shear-like breakup mechanisms very similar to aerodynamic breakup of non-turbulent round liquid jets in gaseous cross flows.

2. Eq. (4) due to Grant and Middleman (1966) provides a reasonable correlation of existing measurements of liquid column breakup lengths for turbulent round liquid jets in still gases due to Chen and Davis (1964), Grant and Middleman (1966) and the present investigation for *We* of 200–100,000. This correlation, however, is influenced by effects of transition toward laminar jet exit conditions and Rayleigh-like liquid column breakup at small *We* and transition to aerodynamic bag/shear breakup at large *We* which provides an explanation for the somewhat weaker dependence of the liquid column breakup length on *We* given by the Grant and Middleman expression, Eq. (4), than for the present correlation for the turbulent breakup mode, Eq. (9), that dominates most of this *We* range.

3. Mean streamwise drop velocities after turbulent primary breakup are essentially identical to mean streamwise velocities within the liquid jet whereas mean cross stream drop velocities after turbulent primary breakup are comparable to cross stream rms velocity fluctuations in the liquid. Mean cross stream drop velocities relative to the liquid surface after turbulent primary breakup near the jet exit, however, are smaller than absolute mean cross stream drop velocities after turbulent primary breakup because effects of cross stream flapping of the liquid jet as a whole are removed.

4. The mean drop mass flux, $\dot{m}''_L$, due to turbulent primary breakup at the liquid surface was correlated in terms of a surface efficiency factor defined as $\varepsilon = \dot{m}''_L/(\rho_L \tilde{v}_r)$ in the same manner as the variation of drop SMD after turbulent primary breakup, Eq. (13). Quite plausibly, ε is small at the onset of turbulent primary breakup but reaches values of the order of magnitude of unity as the end of the liquid core is approached.

Although transition requirements for liquid column breakup, for mean drop velocities after turbulent primary breakup, and for mean liquid mass flux surface efficiency factors are provided as functions of *We* for present test conditions, an underlying requirement is that conditions at the jet exit must be turbulent. In addition, it is known that merging of turbulent primary breakup and

secondary breakup occurs for liquid/gas density ratios smaller than 500, see Wu and Faeth (1993); for such conditions, aerodynamic effects on turbulent primary breakup are likely to differ from the behavior observed during the present investigation and clearly merit additional study due to numerous practical applications involving breakup for relatively small liquid/gas density ratios.

Acknowledgements

The research was supported by the Office of Naval Research, Grant No. N00014-95-1-0234 under the technical management of E.P. Rood. Initial development of research facilities was carried out under Air Force Office of Scientific Research, Grant No. AFOSR F49620-95-1-0364 under the technical management of J.M. Tishkoff. Financial support for one of us (K.A.S.) under the Rackham Fellowship Program of the University of Michigan is also gratefully acknowledged.

References

Chehroudi, B., Onuma, Y., Chen, S.-H., Bracco, F.V., 1985. On the intact core of full cone sprays. SAE Paper No. 850126.

Chen, T.-F., Davis, J.R., 1964. Disintegration of a turbulent water jet. J. Hyd. Div. 1, 175–206.

Chou, W.-H., Faeth, G.M., 1998. Temporal properties of secondary drop breakup in the bag breakup regime. Int. J. Multiphase Flow 24, 889–912.

Chou, W.-H., Hsiang, L.-P., Faeth, G.M., 1998. Temporal properties of drop breakup in the shear breakup regime. Int. J. Multiphase Flow 23, 657–669.

Dai, Z., Faeth, G.M., 2001. Temporal properties of secondary drop breakup in the multimode breakup regime. Int. J. Multiphase Flow 27, 217–236.

Dai, Z., Chou, W.-H., Faeth, G.M., 1998. Drop formation due to turbulent primary breakup at the free surface of plane liquid wall jets. Phys. Fluids 10, 1147–1157.

De Juhasz, K.J., Zahn Jr., O.F., Schweitzer, P.H., 1932. On the formation and dispersion of oil sprays. Bulletin No. 40, Engineering Experimental Station, The Pennsylvania State University, University Park, PA.

Ervine, D.A., Falvey, H.T., 1987. Behavior of turbulent water jets in the atmosphere and in plunge pools. Proc. Inst. Civ. Eng. 83 (Pt. 2), 295–314.

Faeth, G.M., 1996. Spray combustion phenomena. Proc. Combust. Inst. 26, 1593–1612.

Grant, R.P., Middleman, S., 1966. Newtonian jet stability. AIChE J. 12, 669–678.

Hiroyasu, H., Shimizu, M., Arai, M., 1982. The breakup of a high speed jet in a high pressure gaseous environment. ICLASS-82, University of Wisconsin, Madison, WI.

Hoyt, J.W., Taylor, J.J., 1977a. Waves on water jets. J. Fluid Mech. 88, 119–123.

Hoyt, J.W., Taylor, J.J., 1977b. Turbulence structure in a water jet discharging in air. Phys. Fluids 20, S253–S257.

Hsiang, L.-P., Faeth, G.M., 1992. Near-limit drop deformation and secondary breakup. Int. J. Multiphase Flow 18, 635–652.

Hsiang, L.-P., Faeth, G.M., 1995. Drop deformation and breakup due to shock wave and steady disturbances. Int. J. Multiphase Flow 21, 545–560.

Lee, D.W., Spenser, R.C., 1933a. Preliminary photomicrographic studies of fuel sprays. NACA Technical Note 424, Washington, DC.

Lee, D.W., Spenser, R.C., 1933b. Photomicrographic studies of fuel sprays. NACA Technical Note 454, Washington, DC.

Mazallon, J., Dai, Z., Faeth, G.M., 1999. Primary breakup of nonturbulent round liquid jets in gas crossflows. At. sprays 9, 291–311.

McCarthy, M.J., Malloy, N.A., 1974. Review of stability of liquid jets and the influence of nozzle design. Chem. Eng. J. 7, 1–20.

Phinney, R.E., 1973. The breakup of a turbulent jet in a gaseous atmosphere. J. Fluid Mech. 60, 689–701.
Sallam, K.A., Dai, Z., Faeth, G.M., 1999. Drop formation at the surface of plane turbulent liquid jets in still gases. Int. J. Multiphase Flow 25, 1161–1180.
Schweitzer, P.H., 1937. Mechanism of disintegration of liquid jets. J. Appl. Phys. 8, 513–521.
Simmons, H.C., 1977. The correlation of drop-size distributions in fuel nozzle sprays. J. Eng. Power 99, 309–319.
Tennekes, H., Lumley, J.L., 1972. In: A First Course in Turbulence. MIT Press, Cambridge, MA, pp. 248–286.
Townson, J.M., 1988. Free-Surface Hydraulics, first ed. Unwin Hyman, London (Chapter 6).
Weber, C., 1931. Zum zerfall eines flussigkeitsstrahles. Z. Angew. Math. Mech. 2, 136–141.
Wu, P.-K., Faeth, G.M., 1993. Aerodynamic effects on primary and secondary spray breakup. At. Sprays 3, 265–289.
Wu, P.-K., Faeth, G.M., 1995. Onset and end of drop formation along the surface of turbulent liquid jets in still gases. Phys. Fluids A 7, 2915–2917.
Wu, P.-K., Tseng, L.-K., Faeth, G.M., 1992. Primary breakup in gas/liquid mixing layers for turbulent liquids. At. Sprays 2, 295–317.
Wu, P.-K., Miranda, R.F., Faeth, G.M., 1995. Effects of initial flow conditions on primary breakup of nonturbulent and turbulent round liquid jets. At. Sprays 5, 175–196.
Wu, P.-K., Kirkendall, K.A., Fuller, R.P., Nejad, A.S., 1997. Breakup processes of liquid jets in subsonic crossflow. J. Prop. Power 13, 64–73.